

Calculation of energies and hyperfine-structure constants of $^{233}\text{U}^+$ and ^{233}U

S. G. Porsev ¹, C. Cheung ¹ and M. S. Safronova^{1,2}

¹*Department of Physics and Astronomy, University of Delaware, Newark, Delaware 19716, USA*

²*Joint Quantum Institute, National Institute of Standards and Technology and the University of Maryland, College Park, Maryland 20742, USA*



(Received 7 May 2022; accepted 28 September 2022; published 17 October 2022)

We carried out calculations of the energies and magnetic dipole hyperfine-structure constants of the low-lying states of $^{233}\text{U}^+$ and ^{233}U using two different approaches. With six valence electrons and a very heavy core, uranium represents a major challenge for precision atomic theory even using large-scale computational resources. The first approach combines configuration interaction (CI) with a method allowing us to include core-valence correlations to all orders of the perturbation theory over residual Coulomb interaction. The second approach is a pure CI method which allows the use of different initial approximations. We present a detailed analysis of all calculated properties and discuss the advantages and disadvantages of each of these methods. We report a preliminary value of the U nuclear magnetic moment and outline the need for further experiments.

DOI: [10.1103/PhysRevA.106.042810](https://doi.org/10.1103/PhysRevA.106.042810)

I. INTRODUCTION

Experimental measurements of hyperfine structure (hfs) together with theoretical calculations can be used to determine nuclear moments. Recently, we calculated the hfs constants A and B for a heavy ion, $^{229}\text{Th}^{3+}$ [1]. Combining these values with the experimental results, we extracted the magnetic dipole and electric quadrupole nuclear moments with high accuracy. The electronic structure of Th^{3+} , which has a single valence electron, allowed for the most precise calculation for an actinide ion. The 229 isotope of Th has a very small transition energy (≈ 8 eV) between the ground and first excited nuclear states. Due to such a unique feature, this nuclear transition was proposed for the design of a new type of optical clock (see review [2] and references therein).

The Th ions were successfully trapped, and further precision laser spectroscopic investigation of the hyperfine structure is planned [2]. Thorium isomer energy can be measured using the decay of the isomer state in neutral Th via internal conversion [3]. In these experiments, ^{229}Th isomer is produced from the α decay of ^{233}U . As a result, one can investigate the hyperfine-structure constants of $^{233}\text{U}^+$ in the same set of experiments. Such an experimental study was carried out in Ref. [4] and the hfs constant A of the first excited state $5f^3 6d7s \ ^6L_{11/2}$ was found with about 2% uncertainty to be $-301(6)$ MHz. Therefore, an accurate calculation of this constant can potentially lead to improving the current value of the nuclear magnetic moment $\mu = 0.59(5) \mu_N$ [5] (where μ_N is the nuclear magneton), known with only 8.5% accuracy.

Motivated by these and future experiments, we carried out calculations of the energies and magnetic dipole hfs constants A of the low-lying states of $^{233}\text{U}^+$ and ^{233}U . The U^+ ions and neutral U are very challenging systems for precision atomic calculations. First, these are heavy atomic systems with the nuclear charge $Z = 90$. Second, the main configurations of the ground states of U^+ and U are $5f^3 6d7s$ and $5f^3 6d7s^2$, respectively. These five or six electrons can be considered as the valence electrons, while all the rest can be treated as the core. Numerous problems that occur in calculating the hfs constants for neutral uranium were discussed in the recent paper [6].

An accurate treatment of both valence-valence and core-valence correlations in actinides with many valence electrons is a very challenging task that is currently unsolved. In this paper, we explore its possible solutions, using two different methods. The first one is a combination of the configuration-interaction (CI) method with a method allowing us to include core-valence correlations in the second order or all orders of the perturbation theory over residual Coulomb interaction [7,8]. This method proved to be very efficient for calculating energies of the low-lying levels of both the singly charged and neutral uranium. The transition energies were reproduced with an accuracy of several tens of cm^{-1} . This is the most accurate calculation carried out so far in such a system to the best of our knowledge. However, we found unexpected difficulties when computing hfs constants of the excited states of U^+ : unusually large core-valence correlation corrections to the expectation values of the magnetic dipole hyperfine operator. Performing a full-scale calculation in the framework of the pure CI method with a different initial approximation allowed us to circumvent this problem. In this method, we consider only valence-valence correlations, while core-valence correlations are not taken into account explicitly. The latter can be considered as a drawback of this method, but on the other hand we have the freedom to choose an optimal initial approximation,

Published by the American Physical Society under the terms of the [Creative Commons Attribution 4.0 International license](https://creativecommons.org/licenses/by/4.0/). Further distribution of this work must maintain attribution to the author(s) and the published article's title, journal citation, and DOI.

obtained from the Dirac-Hartree-Fock (DHF) self-consistency procedure. The advantages and disadvantages of these methods and the results obtained within each of them will be discussed in detail in the following sections.

II. CI + MBPT AND CI+ ALL-ORDER METHODS OF CALCULATION

We consider U^+ and U as the atomic systems with a $[1s^2, \dots, 6p^6]$ core and five and six valence electrons above it, respectively. The initial DHF self-consistency procedure included the Breit interaction and was done for the core electrons; such potential is usually denoted V^{N-M} , where N is the total number of electrons and M is the number of valence electrons. The advantage of such potential is the easiest formulation of the perturbation theory and coupled-cluster (all-order) approaches without the appearance of the large so-called subtraction diagrams (see detailed discussion in Ref. [9]).

The only successful attempt to use a different starting potential with a CI+ all-order method, when the initial approximation did not correspond to the self-consistent field of the core, was for Pb, where the V^{N-M} starting potential was used to treat the system with four valence electrons [9]. However, Pb had a special case of a closed $6s^2$ shell, and no such analog potential can be constructed for U and U^+ .

In U^+ and U , the only potential with which we can use the CI+ all-order method is $V^{N-5(6)}$ for U^+ and U , respectively. However, increasing M leads to degrading quality of the one-electron orbitals and a much larger number of configurations that have to be included in CI. The $5f$, $7s$, $6d$, and $7p$ orbitals were constructed in such a frozen-core potential. The remaining virtual orbitals were formed using 40 basis set B-spline orbitals. The basis set included partial waves with the orbital quantum number up to $l = 6$. Quantum electrodynamic (QED) corrections were also included following Refs. [10,11].

In an approach combining CI and a method allowing us to include core-valence correlations [7,8], the wave functions and energy levels of the valence electrons were found by solving the multiparticle relativistic equation [7]:

$$H_{\text{eff}}(E_n)\Phi_n = E_n\Phi_n, \quad (1)$$

where the effective Hamiltonian is defined as

$$H_{\text{eff}}(E) = H_{\text{FC}} + \Sigma(E), \quad (2)$$

with H_{FC} being the Hamiltonian in the frozen-core approximation. The energy-dependent operator $\Sigma(E)$ accounts for virtual excitations of the core electrons. We constructed it in two ways: using (i) the second-order many-body perturbation theory (MBPT) over residual Coulomb interaction [7] and (ii) the linearized coupled-cluster single-double method [8,12]. In the following, we refer to these approaches as the CI + MBPT and CI+ all-order methods.

To check the convergence of the CI, we have performed several calculations, sequentially increasing the size of the configuration space. For U^+ , the smallest set of the configurations was constructed by including the single and double excitations from the main configurations of the low-lying states to the shells up to $13s$, $13p$, $13d$, $13f$, and $13g$ (we

designate it as $[13spdfg]$). We have identified seven configurations the weight (in probability) of which exceeded 3% for all states of interest to be $5f^37s^26d$, $5f^37s6d$, $5f^37s8s$, $5f^36d8s$, $5f^37s7d$, $5f^27s6d6f$, and $5f^27s^26f$. All subsequent (larger) sets of configurations were constructed by allowing single and double excitations from these seven configurations. The largest set of configurations, for which the saturation was practically reached, included the single and double excitations to $[20spd17f13g]$ orbitals.

The same approach was used for constructing sets of configurations for neutral U . The single and double excitations were allowed from the configurations the weight of which exceeded 3%. For U , the largest set of configurations $[20spd17f13g]$ included 131×10^6 determinants.

A. Energy levels

The excitation energies of the lowest-lying states of U^+ and U obtained in different approximations are listed (in cm^{-1}) in Table I. The assignments of the U^+ and U levels are from Ref. [13] and the NIST database [14], respectively.

In the third column, we present the CI + MBPT values. They were obtained only for the $[13spdfg]$ set of configurations to demonstrate the size of the higher-order core-valence corrections. In columns 4–7, we present the CI+ all-order values for different sets of configurations. We find that the transition energies are not very sensitive to the size of the configuration space. They change only slightly (by several tens of cm^{-1}) when the set of configurations is increased from $[13spdfg]$ to $[20spd17f13g]$. Following Ref. [11], we calculated the QED corrections to the energy levels. They are listed in the column labeled “QED.” The final values, given in the column labeled “Final,” are the sum of the CI+ all-order values obtained for the $[20spd17f13g]$ configuration set and the QED correction. We see excellent agreement between the theoretical and experimental values. Even for the small transition energy between the ground state of U^+ and the first excited state ${}^6L_{11/2}$, which is 289 cm^{-1} , the difference between the theory and experiment is only at the level of 5%. We also note that the main configuration of the ground state is $5f^37s^2$ while the main configuration of the excited states is $5f^36d7s$. Thus, we reproduce equally well the energies of the states belonging to the different configurations.

B. Magnetic dipole hyperfine-structure constants

The hfs coupling due to nuclear multipole moments may be represented as a scalar product of two tensors of rank k :

$$H_{\text{hfs}} = \sum_k (\mathbf{N}^{(k)} \cdot \mathbf{T}^{(k)}),$$

where $\mathbf{N}^{(k)}$ and $\mathbf{T}^{(k)}$ act in the nuclear and electronic coordinate space, respectively. In the following, we restrict ourselves to the first term in the sum over k , considering only the interaction of the magnetic dipole nuclear moment with the electrons, i.e.,

$$H_{\text{hfs}} \approx \mathbf{N}^{(1)} \cdot \mathbf{T}^{(1)} \equiv \mathbf{N} \cdot \mathbf{T}.$$

TABLE I. The excitation energies (in cm^{-1}), calculated in the CI+MBPT and CI+all-order approximations, are presented. The CI+all-order values are listed for different sets of configurations. The QED corrections are given in the column labeled “QED.” The final values, given in the column labeled “Final,” are found as the sum of the CI+all-order values obtained for the $[20spd17f13g]$ configuration set and the QED corrections. The experimental values are given in the last two columns.

Level	CI+MBPT		CI+all-order				QED	Final	Expt.	
	$[13spdfg]$	$[13spdfg]$	$[15spdf13g]$	$[17spdf13g]$	$[20spd17f13g]$	Ref. [13]			Ref. [14]	
U^+ $5f^37s^2\ ^4I_{9/2}$	0	0	0	0	0	0	0	0	0	0
$5f^36d7s\ ^6L_{11/2}$	1411	497	498	409	450	-175	274	289		
$5f^36d7s\ ^6K_{9/2}$	1896	1088	1088	1003	1033	-170	862	915		
$5f^36d7s\ ^6L_{13/2}$	3008	2006	2005	1907	1934	-188	1746	1749		
$5f^36d7s\ ^6K_{11/2}$	3382	2471	2470	2377	2396	-180	2215	2295		
U $5f^36d7s^2\ ^5L_6$	0	0	0	0	0	0	0	0		0
$5f^36d7s^2\ ^5L_7$	4420	3772	3779	3775	3784	8	3792			3801
$5f^36d7s^2\ ^5K_6$	4757	4221	4231	4225	4225	10	4235			4276

We define \mathbf{N} in a dimensionless form, expressing it through the nuclear magnetic dipole moment $\boldsymbol{\mu}$ as

$$\mathbf{N} = \boldsymbol{\mu}/\mu_N.$$

The operator \mathbf{T} is the sum of the one-particle operators:

$$\mathbf{T} = \sum_{i=1}^N \mathbf{T}_i.$$

Assuming the nucleus to be a charged ball of uniform magnetization with radius R , the expression for one-particle electronic tensor \mathbf{T}_i is given (in atomic units $\hbar = |e| = m = 1$, $c \approx 137$) by

$$\mathbf{T}_i = \frac{\mathbf{r}_i \times \boldsymbol{\alpha}_i}{c r_i^3} \mu_N,$$

where $\boldsymbol{\alpha}_i$ is the Dirac matrix, r_i is the radial position of the i th electron, $\mathbf{r}_i \times \boldsymbol{\alpha}_i$ is the vector product of \mathbf{r}_i and $\boldsymbol{\alpha}_i$, and

$$r_i > \equiv \begin{cases} r_i, & \text{if } r_i \geq R, \\ R, & \text{if } R > r_i. \end{cases} \quad (3)$$

The formula connecting the hfs constant A of an atomic state $|\gamma J\rangle$ with the reduced matrix element $\langle \gamma J || T || \gamma J \rangle$ of the electronic tensor \mathbf{T} is

$$A = \frac{g_N}{\sqrt{J(J+1)(2J+1)}} \langle \gamma J || T || \gamma J \rangle,$$

where γ encapsulates all other quantum numbers, $g_N = \mu/(\mu_N I)$, and I is the nuclear spin.

We determine the hfs constants A for the low-lying states of the neutral and singly ionized uranium. For these calculations, we use the value of the nuclear magnetic moment of ^{233}U , $\mu = 0.59(5)\mu_N$ [5] ($I = 5/2$). We note that its uncertainty, 8.5%, is large.

The results of several computations demonstrating the size of various contributions are summarized in Table II. In the third column, we present the results obtained at the CI+MBPT stage, when the core-valence correlations are included in the second order of the perturbation theory. The CI+all-order results that include higher-order core-valence correlations are obtained for the largest $[20spd17f13g]$ set of configurations. These values are given in the fourth column.

The correlation corrections to the hfs expectation values arise from the correlation corrections to the wave functions and the corrections to the hfs operator. The most important and (often) the largest one is the random-phase approximation (RPA) correction, which is calculated in all orders of the perturbation theory and given separately in the table in the column labeled “RPA.” We also took into account other corrections to the hfs operator: the two-particle (2P) and core Brueckner (σ) [17], and the structural radiation (SR) [18,19], QED, and normalization (Norm.) corrections. They are listed in the respective columns. Representative diagrams for the 2P, σ , and SR corrections are shown in Fig. 1.

Thus, the 2P correction appears already in the first order of the perturbation theory, while the σ and SR corrections appear in the second order of MBPT. As illustrated in Table II, the 2P corrections are very large for all excited states for U^+ . For instance, this correction is more than 100% of the “CI+All” value for the $^6L_{11/2}$ and $^6K_{9/2}$ states, which is very unusual. We had not observed it earlier for any other system. On the other hand, the CI+all-order method has not been applied before to compute hfs for such a complicated system. The calculations of the U^+ properties were practically not carried out before, and specific features of these particular states are little studied. Our finding raises the question of the applicability of the perturbation theory for calculating this correction. We can expect that higher-order corrections will play an essential role and can significantly change the hfs constants values for the excited states. Therefore, the current results obtained for these states have low accuracy, estimated to be about 50%.

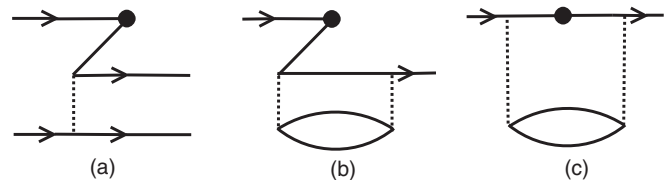


FIG. 1. Representative diagrams for (a) the two-particle correction, (b) the core Brueckner correction, and (c) the structural radiation correction. A filled circle stands for the hfs operator and a dotted line stands for the Coulomb interaction.

TABLE II. Contributions to the magnetic dipole hfs constants A (in MHz), calculated with $\mu = 0.59 \mu_N$, are presented. The CI+MBPT and CI+all-order values are listed in the columns labeled “CI+MBPT” and “CI+All,” respectively. The RPA corrections to the hfs operator are listed in the column labeled “RPA.” The core Brueckner (σ), structural radiation (SR), two-particle (2P), QED, and normalization (Norm.) corrections are given in respective columns and summarized in the column labeled “Tot. corr.” The values in the column labeled “Final” are obtained as the sum of the “CI+All” + “RPA” + “Tot. corr.” values. Uncertainties are given in parentheses.

		CI+MBPT	CI+All	RPA	σ	SR	2P	QED	Norm.	Tot. corr.	Final	Expt.
U ⁺	$A(5f^3 7s^2 \ ^4I_{9/2})$	150	140	-2	3	31	-4	-3	-29	-1	137(10)	
	$A(5f^3 6d7s \ ^6L_{11/2})$	-128	-120	-26	27	37	-162	6	43	-50	-196	-301(6) ^a
	$A(5f^3 6d7s \ ^6K_{9/2})$	-173	-157	-7	30	26	-193	11	52	-73	-237	
	$A(5f^3 6d7s \ ^6L_{13/2})$	369	344	33	-16	34	135	-2	-95	56	432	
	$A(5f^3 6d7s \ ^6K_{11/2})$	399	369	46	-19	27	145	-3	-102	48	463	
U	$A(5f^3 6d7s^2 \ ^5L_6)$	125	121	5	4	37	-3	0.9	-30	8	134	131.56(10) ^b
	$A(5f^3 6d7s^2 \ ^5L_7)$	127	122	-18	1	28	3	0.4	-24	9	113	122 ^c
	$A(5f^3 6d7s^2 \ ^5K_6)$	129	124	-10	1	23	3	0.4	-25	2	116	128 ^c

^aReference [4].

^bReference [15].

^cObtained using the results of Ref. [16] and the ratio $A(^{233}\text{U})/A(^{235}\text{U}) \approx -2.1722$ [see Eq. (4) and the discussion after it].

For the ground state $5f^3 7s^2 \ ^4I_{9/2}$, in contrast, the situation is much better. The 2P correction is small. We assume that it can be due to the $7s$ shell being closed and that it does not contribute to the hfs constant. Besides that, all corrections beyond RPA tend to cancel each other. As a result, the total correction, labeled in Table II as “Tot. corr.,” and found as the sum of σ , SR, 2P, QED, and normalization corrections, is small ($\approx 0.7\%$). Estimating the uncertainty of $A(^4I_{9/2})$ as the difference between the “CI+All” and “CI + MBPT” values, we arrive at $A(^4I_{9/2}) = 137(10)$ MHz.

For the neutral uranium, there is good agreement (about 2%) for the hfs constant of the ground state $A(^5L_6)$, while for the excited states 5L_7 and 5K_6 the agreement is at the level of 10%. Same as for the ground state of U⁺, the corrections to the hfs constants are not very large and tend to cancel each other. The 2P corrections are small, which again can be explained by the presence of the closed $7s$ shell.

We note that the experimental values $A(^5L_7) = -56.31(12)$ MHz and $A(^5K_6) = -59.13(45)$ MHz are known with high accuracy for ^{235}U [16], but they were not measured for ^{233}U . In Ref. [15] the magnetic dipole hfs constants of the ground state ($5f^3 6d7s^2 \ ^5L_6$) and two even-parity states ($5f^3 6d7s7p \ ^7M_7$, $E = 16\,900 \text{ cm}^{-1}$) and ($5f^3 6d7s7p \ ^7L_6$, $E = 17\,362 \text{ cm}^{-1}$) were measured for both ^{233}U and ^{235}U .

Their ratios were found in Ref. [15] to be

$$\begin{aligned}
 A_{5L_7}(^{233}\text{U})/A_{5L_7}(^{235}\text{U}) &= -2.1656(16), \\
 A_{7M_7}(^{233}\text{U})/A_{7M_7}(^{235}\text{U}) &= -2.1790(10), \\
 A_{7L_6}(^{233}\text{U})/A_{7L_6}(^{235}\text{U}) &= -2.172(14).
 \end{aligned} \tag{4}$$

As seen, the values of these ratios are very close to each other; the largest difference between -2.1790 and -2.1656 is only about 0.6%. This is not surprising because the electronic matrix elements $\langle \gamma J || T || \gamma' J \rangle$ are practically the same for both ^{233}U and ^{235}U . A small difference in nuclear radii affects the ratio of these matrix elements very little.

Using the average of the three ratios given in Eq. (4), -2.1722 , and assuming that this is about the same also for the hfs constants of the $^6L_{11/2}$ and $^6K_{9/2}$ states, we found the

respective values $A(^6L_{11/2})$ and $A(^6K_{9/2})$, presented in the last column of Table II.

III. PURE CI CALCULATIONS

One of the reasons for the low accuracy of the hfs constants of the excited states of U⁺ is a poor initial approximation. Indeed, the initial DHF self-consistency procedure was done for the core [$1s^2, \dots, 6s^2, 6p^6$] electrons. Then the valence orbitals were constructed in the frozen-core approximation, i.e., in the field of the sixfold ionized neutral atom, whereas we would be interested in constructing orbitals for the neutral atom. In this section, we discuss another (pure CI) method of calculation that allows us to use a much better initial approximation. The role of the core-valence correlations can be estimated by successively adding the core shells ($6p$, $6s$, etc.) to the valence field and by calculating the hfs constants for these extended CI spaces. Such a method is similar to the multiconfiguration Dirac-Hartree-Fock (MCDHF) variational approach [20]. In particular, in this review paper the authors discuss an optimization strategy for choosing orbitals that should be involved in the MCDHF process.

Again, at first U⁺ and U were considered as the atomic systems with five and six valence electrons, respectively, above the closed core [$1s^2, \dots, 6p^6$]. But this time, we solved the DHF equations in the V^N approximation for both atomic systems, i.e., the initial self-consistency procedure was carried out for the [$1s^2, \dots, 6p^6, 5f^3 6d 7s$] configuration for U⁺ and for the [$1s^2, \dots, 6p^6, 5f^3 6d 7s^2$] configuration for U. For U⁺, all electrons were frozen, the electron from the $6d$ shell was moved to the $7p$ shell, and the $7p_{1/2,3/2}$ orbitals were constructed in the frozen-core potential. The remaining virtual orbitals were formed using a recurrent procedure described in Refs. [21,22]. The newly constructed orbitals were then orthonormalized with respect to the orbitals of the same symmetry.

For both atomic systems, the basis sets included in total five partial waves ($l_{\max} = 4$) and the orbitals with the principal quantum number n up to 20. We included the Breit interaction on the same footing as the Coulomb interaction when constructing the basis set.

TABLE III. Magnetic dipole hfs constants A (in MHz) of the $5f^3 6d7s \ ^6L_{11/2}$ state of U^+ , obtained in different approximations with $\mu = 0.59 \mu_N$, are presented. The experimental value is given in the last column. The final theoretical value is given in the row labeled "Final." Uncertainties are given in parentheses.

	[7spdf]	[8spdf]	[8spdf6g]	[9spdf]	[10spdf]	[11spdf]	[12spdf]	[13spdf]	Expt. [4]
5e CI	-234	-264	-272	-264	-263	-263	-263	-263	-301(6)
11e CI	-237	-283	-283	-289	-286	-285	-286	-287	
13e CI	-242	-297	-292	-315	-310	-301	-296	-296	
23e CI	-249.6	-291	-288	-313	-311				
29e CI	-250.9	-294	-295	-323					
31e CI	-250.6	-284							
Final					-298(10)				

We note that with such a construction of the basis set the number of electrons included in the DHF self-consistent procedure differs from the number of the core electrons. As discussed earlier, we cannot use the CI+ all-order method with such a starting potential. So, we apply the pure CI method, accounting for explicitly only the valence-valence correlations but considering more and more electrons as the valence electrons in successive approximations.

A. The hfs constant A of the ($5f^3 6d7s \ ^6L_{11/2}$) state for U^+

Our goal is to calculate the hfs constant A of the first excited state ($5f^3 6d7s \ ^6L_{11/2}$) (for which the experimental value is known) in the framework of the pure CI method. At first, we consider U^+ as the ion with five valence electrons and, respectively, we do five-electron CI (in the following, we designate it as 5e CI).

We construct the sets of configurations by allowing single and double excitations of electrons from the two main configurations $5f^3 7s^2$ and $5f^3 7s6d$ to higher-lying orbitals. We successively increased the configuration space, following the change of the constant A , until it stops changing. The largest set of configurations was constructed by single and double excitations to [13spdf]. The results obtained for 5e CI for different sets of configurations are given in the first row of Table III. As seen, practically the same values were found for the [10, 11, 12, 13spdf] sets of configurations.

As a next step, we estimated the role of the core-valence correlations by successively including the $6p$, $6s$, and $5d$ shells in the valence field and carrying out calculations in the framework of 11-, 13-, and 23-electron CI, respectively. The results obtained for different sets of configurations are presented in rows 2–4 in Table III.

Finally, we included the $5p$ and $5s$ shells in the valence field and carried calculations in the framework of 29e CI and 31e CI. The largest set of configurations for 29e CI was [9spdf] while for 31e CI it was [8spdf]. Due to a very large number of determinants we are unable to carry out calculation for [9spdf] in the framework of 31e CI, but we can do the following estimate. The contribution from the excitations to the $9spdf$ shells for 29e CI can be determined as $A([9spdf]) - A([8spdf]) = -29$ MHz. Assuming that the contribution from the excitations to the $9spdf$ shells for 31e CI is comparable, we would obtain for 31e CI the value of the constant $A[9spdf] \simeq -313$ MHz which is close to the value

obtained for 23e CI. Thus, when we include the $5p$ and $5s$ shells in the CI space, their contributions to the constant A tend to cancel each other.

To find out the role of excitations to the g shells we compared the results for [8spdf] and [8spdf6g]. They are given in Table III in columns 3 and 4. For different sets of configurations we observe that the excitations to the $5g$ and $6g$ shells change the hfs constant at the level of few MHz. For the 29e CI the difference $A([8spdf6g]) - A([8spdf]) = -1$ MHz. We also checked that the excitations to the $7g$ – $10g$ shells, practically, do not play any role. They lead to a change of the constant A by less than 1 MHz.

As we observed for 11e and 13e CIs, the CI spaces were saturated for the [13spdf] set of configurations. We consider the value -296 MHz, obtained for 13e CI for the [13spdf] set of configuration, as closest to the final result. To estimate corrections to this value due to contributions of the deeper-lying core shells, we added the difference $A(23e \text{ CI}) - A(13e \text{ CI}) = -1$ MHz, found for the [10spdf] set of configurations, and also the difference $A([8spdf6g]) - A([8spdf]) = -1$ MHz found for 29e CI, to -296 MHz, arriving at -298 MHz. As we already mentioned, the excitations from the $5p$ and $5s$ shells give contributions to the constant A tending to cancel each other.

We were unable to include into consideration the excitations from the $1s, \dots, 4d$ core shells. But they are lying already sufficiently deep (e.g., the DHF energy of the $4d_{5/2}$ orbital is -28 a.u.). We believe that the total contribution from excitations from these shells to the final value of the hfs constant A does not exceed the difference between the results, obtained for [9spdf] for 29e CI and 23e CI, equal to 10 MHz. We consider this value as the uncertainty of our calculation.

Using the theoretical and experimental values for $A(^6L_{11/2})$, $-298(10)$, and $-301(6)$ MHz [4], respectively, we are able to extract the nuclear magnetic moment of $^{233}\text{U}^+$ to be $\mu/\mu_N \approx 0.596(24)$. We note that this value is somewhat inconclusive because we used only one hfs constant. Further experimental measurements of other hfs constants of the low-lying states are needed. By performing similar calculations and analyses for these constants, we would be able to refine the value of the magnetic moment. Besides that, it would allow us to investigate the problem of the Bohr-Weisskopf effect of the finite nuclear magnetization, which is omitted in the present calculation due to the lack of further

TABLE IV. Magnetic dipole hfs constants A (in MHz) of the four lowest-lying states of ^{233}U obtained (with $\mu = 0.59 \mu_N$) in the framework of $6e$ CI in different approximations. The experimental values are given in the last column.

		[7 <i>spdfg</i>]	[8 <i>spdfg</i>]	[10 <i>spd8fg</i>]	[11 <i>sp10dfg</i>]	Expt.
6 <i>e</i> CI	$A(5f^3 6d7s^2 \ ^5L_6)$	134	107	114	115	131.56(10) ^a
	$A(5f^3 6d7s^2 \ ^5L_7)$	136	125	126	126	122 ^b
	$A(5f^3 6d7s^2 \ ^5K_6)$	40	123	123	124	128 ^b
	$A(5f^3 6d^2 7s \ ^7M_6)$	-39	-135	-144	-144	-147 ^b

^aReference [15].

^bRecalculated from the results presented in Ref. [16].

experimental values that will allow its extraction (see Ref. [1] for details). We note that if the nuclear magnetic moment of ^{233}U is known with good accuracy and also knowing the highly accurate value of the ratio of the nuclear magnetic moments $\mu(^{233}\text{U})/\mu(^{235}\text{U}) = 1.5604(14)$ [5,23] we are able to determine the nuclear magnetic moment of ^{235}U .

B. The hfs constants A of the low-lying states of U

An accurate calculation of different properties of the neutral uranium is generally a more complicated task due to an extra valence electron in comparison to U^+ . We consider U as the atom with six valence electrons and, respectively, we do the six-electron CI, constructing the configurations by allowing single and double excitations from the two main configurations $5f^3 7s^2 6d$ and $5f^3 7s 6d^2$ to higher-lying orbitals. The results are presented in Table IV. As seen from the table, the results obtained for the [10*spd8fg*] and [11*sp10dfg*] sets of configurations are very close to each other for all four considered states. So we can say that the saturation of $6e$ CI is achieved. The values of the hfs constants are in reasonable agreement with the experimental data. Unfortunately, a reliable calculation of the hfs constants in the framework of $12e$ CI (when the $6p$ shell was included in the valence field) proved impossible even with modern computer capabilities. Even for a rather small [7*spdfg*] set of configurations, the CI space consisted of 84×10^6 determinants.

IV. CONCLUSION

In summary, we carried out calculations of the energy levels and hfs constants for a number of the low-lying states of U^+ and U in the framework of the CI+ all-order and pure CI methods. Using the calculated and experimental results of the

magnetic dipole hfs constant $A(^6L_{11/2})$ of U^+ , we extracted the value of the magnetic dipole moment μ_N of the nucleus of ^{233}U . Further experimental measurements of other magnetic dipole hfs constants of the low-lying states and accurate theoretical calculations are needed to confirm the value of μ_N obtained in this paper.

In the framework of the CI+ all-order method, we calculated the corrections to the hfs operator in the second order of the perturbation theory. For the hfs constants of the excited states of U^+ , these corrections are large, leading to large uncertainties of these values. To be more certain about these quantities, their calculation in all orders of the perturbation theory is required.

In terms of the experiment, a measurement of the magnetic dipole hfs constant A of the ground state ($5f^3 7s^2 \ ^4I_{9/2}$) of $^{233}\text{U}^+$, as well as a direct measurement of the hfs constants of low-lying states of the neutral ^{233}U , such as ($5f^3 6d7s^2 \ ^5L_7$) and ($5f^3 6d7s^2 \ ^5K_6$), would be very useful. This would contribute to further development of the theory, and a better understanding of the possibilities of modern methods of high-precision calculations, and would allow an accurate extraction of U nuclear moments.

ACKNOWLEDGMENTS

This work is a part of the ‘‘Thorium Nuclear Clock’’ project that has received funding from the European Research Council under the European Union’s Horizon 2020 research and innovation program (Grant No. 856415). This work was supported in part by NSF Grant No. PHY-2012068 and through the use of UDEL Caviness and DARWIN computing systems [24].

-
- [1] S. G. Porsev, M. S. Safronova, and M. G. Kozlov, *Phys. Rev. Lett.* **127**, 253001 (2021).
- [2] E. Peik, T. Schumm, M. Safronova, A. Pálffy, J. Weitenberg, and P. Thirolf, *Quantum Sci. Technol.* **6**, 034002 (2021).
- [3] B. Seiferle, L. von der Wense, P. V. Bilous, I. Amersdorffer, C. Lemell, F. Libisch, S. Stellmer, T. Schumm, C. E. Düllmann, A. Pálffy, and P. G. Thirolf, *Nature (London)* **573**, 243 (2019).
- [4] J. Thielking, Ph.D. thesis, Leibniz University, 2020.
- [5] N. J. Stone, *At. Data Nucl. Data Tables* **90**, 75 (2005).
- [6] I. M. Savukov, *Phys. Rev. A* **102**, 042806 (2020).
- [7] V. A. Dzuba, V. V. Flambaum, and M. G. Kozlov, *Phys. Rev. A* **54**, 3948 (1996).
- [8] M. S. Safronova, M. G. Kozlov, W. R. Johnson, and D. Jiang, *Phys. Rev. A* **80**, 012516 (2009).
- [9] S. G. Porsev, M. G. Kozlov, M. S. Safronova, and I. I. Tupitsyn, *Phys. Rev. A* **93**, 012501 (2016).
- [10] V. M. Shabaev, I. I. Tupitsyn, and V. A. Yerokhin, *Phys. Rev. A* **88**, 012513 (2013).
- [11] I. I. Tupitsyn, M. G. Kozlov, M. S. Safronova, V. M. Shabaev, and V. A. Dzuba, *Phys. Rev. Lett.* **117**, 253001 (2016).
- [12] M. G. Kozlov, *Int. J. Quantum Chem.* **100**, 336 (2004).

- [13] J. Blaise, J.-F. Wyart, J. Vergès, R. Engleman, B. A. Palmer, and L. J. Radziemski, *J. Opt. Soc. Am. B* **11**, 1897 (1994).
- [14] Yu. Ralchenko, A. Kramida, J. Reader, and the NIST ASD Team (2011), NIST Atomic Spectra Database, version 4.1, available at <http://physics.nist.gov/asd>, National Institute of Standards and Technology, Gaithersburg, MD.
- [15] Yu. P. Gangrskii, S. G. Zemlyanoi, N. N. Kolesnikov, B. K. Kuldjanov, K. P. Marinova, and B. N. Markov, *Opt. Spectrosc.* **83**, 191 (1997).
- [16] R. Avril, A. Ginibre, and A. Petit, *Z. Phys. D* **29**, 91 (1994).
- [17] V. A. Dzuba, M. G. Kozlov, S. G. Porsev, and V. V. Flambaum, *Zh. Eksp. Teor. Fiz.* **114**, 1636 (1998) [*Sov. Phys. JETP* **87**, 885 (1998)].
- [18] V. A. Dzuba, V. V. Flambaum, P. G. Silvestrov, and O. P. Sushkov, *J. Phys. B* **20**, 1399 (1987).
- [19] S. A. Blundell, W. R. Johnson, Z. W. Liu, and J. Sapirstein, *Phys. Rev. A* **40**, 2233 (1989).
- [20] C. Froese Fischer, M. Godefroid, T. Brage, P. Jönsson, and G. Gaigalas, *J. Phys. B: At. Mol. Opt. Phys.* **49**, 182004 (2016).
- [21] M. G. Kozlov, S. G. Porsev, and V. V. Flambaum, *J. Phys. B: At. Mol. Opt. Phys.* **29**, 689 (1996).
- [22] M. G. Kozlov, S. G. Porsev, M. S. Safronova, and I. I. Tupitsyn, *Comput. Phys. Commun.* **195**, 199 (2015).
- [23] Yu. P. Gangrskii, S. G. Zemlyanoi, B. K. Kuldjanov, K. P. Marinova, and B. N. Markov, *Izv. Akad. Nauk SSSR, Ser. Fiz.* **54**, 830 (1990) [*Bull. Acad. Sci. USSR, Phys. Ser.* **54**, 13 (1990)].
- [24] R. Eigenmann, B. E. Bagozzi, A. Jayaraman, W. Totten, and C. H. Wu, DARWIN: A Resource for Computational and Data-Intensive Research at the University of Delaware and in the Delaware Region, University of Delaware, Newark, DE, 2021, <https://udspace.udel.edu/handle/19716/29071>.